

UC Davis

UC Davis Previously Published Works

Title

Do rearing salmonids predictably occupy physical microhabitat?

Permalink

<https://escholarship.org/uc/item/3728h6db>

Journal

Journal of Ecohydraulics, 5(2)

ISSN

2470-5357

Authors

Moniz, Peter J
Pasternack, Gregory B
Massa, Duane A
[et al.](#)

Publication Date

2020-07-02

DOI

10.1080/24705357.2019.1696717

Peer reviewed

1 Do rearing salmonids predictably occupy physical microhabitat?

2

3 Authors: Peter J. Moniz^{a*}, Gregory B. Pasternack^a, Duane A. Massa^b, Loren W.

4 Stearman^c, and Paul M. Bratovich^d

5

6 Affiliations:

7 ^aDepartment of Land, Air, and Water Resources, University of California at Davis,

8 Davis, CA, USA

9 ^bPacific States Marine Fisheries Commission, Marysville, CA, USA

10 ^cDepartment of Biological Sciences, University of Southern Mississippi, Hattiesburg,

11 MS, USA

12 ^dHDR, Inc., Folsom, CA, USA

13

14 *Corresponding author: pjmoniz@ucdavis.edu

15

16

17

18

19

20

21

22

23 Citation: Moniz, P.J., Pasternack, G.B., Massa, D.A., Stearman, L.W., Bratovich, P.M.

24 2019. Do rearing salmonids predictably occupy physical microhabitat? Journal of

25 Ecohydraulics, doi: 10.1080/24705357.2019.1696717.

26 **Abstract**

27 Microhabitat suitability models are commonly used to estimate salmonid habitat
28 abundance and quality with unknown accuracy or reliability. When tested, the metrics
29 used to evaluate these models are often limited by the methods used to develop them.
30 More generalized bioverification strategies that transcend methodology are therefore
31 needed in ecohydraulics. This study further developed and applied such a generalized
32 bioverification framework to four approximately 1-m-resolution rearing salmonid
33 microhabitat suitability models. Water depth and velocity habitat suitability criteria
34 (HSC) functions were developed for two size classes of rearing *Oncorhynchus*
35 *tshawytscha* and *O. mykiss* using snorkel survey data collected over three years at seven
36 sites along the lower Yuba River in California, USA. An expert-based cover HSC
37 function was modified from previous studies. HSC functions were applied to previously
38 validated, approximately 1-m-resolution two-dimensional hydrodynamic models and
39 cover maps of the river. Mann-Whitney U tests confirmed that suitability values were
40 significantly higher at utilized locations compared to randomly-generated, non-utilized
41 locations for all four models. Bootstrapped forage ratios demonstrated that microhabitat
42 suitability models accurately predicted both preferred and avoided habitat beyond the
43 95% confidence level. This generalized bioverification framework is recommended for
44 evaluating and comparing the accuracy and reliability of ecohydraulic models used in
45 habitat management worldwide.

46 Keywords: microhabitat suitability model, aquatic habitat; salmonid habitat;
47 rearing habitat; two-dimensional hydrodynamic model

48

49 **Introduction**

50 Aquatic ecosystems worldwide have experienced a long history of anthropogenic
51 impacts, including flow regulation, channel simplification, modification of sediment
52 supply, and water quality alterations (Meybeck 2003). One way resource managers have
53 analysed and attempted to mitigate these impacts is through the use of ecohydraulic
54 modelling. These models typically evaluate how changes in discharge, substrate, and/or
55 channel topography relate to the abundance and quality of available aquatic habitat
56 (Lamouroux et al. 1998; Waddle 2001; Lamb et al. 2004). Although ecohydraulic
57 models have largely been used for dam management over the last half-century (Tharme
58 2003), they have increasingly been used for other applications, such as habitat
59 restoration (Pasternack et al. 2004; Gard 2006, 2014; Schwindt et al. 2019), land use
60 and climate change assessment (Guse et al. 2015), and urban river management (Anim
61 et al. 2018).

62 A specific method commonly used in ecohydraulic modelling is the microhabitat
63 suitability model, where spatially explicit point-scale values of physical attributes (e.g.,
64 water depth, velocity, substrate, cover, etc.) are assigned relative indices of habitat
65 quality (i.e., suitability values), typically ranging from 0 (least suitable) to 1 (most
66 suitable) (Bovee 1986). One- and two-dimensional (1D and 2D) hydrodynamic models
67 are commonly used to predict and map the spatial distribution of water depth and
68 velocity values within a study domain (Gibson and Pasternack 2015), while substrate
69 and cover features are mapped from field surveys and/or remote sensing (Arif et al.
70 2017; Lallias-Tacon et al. 2017). Biological models are then used to relate these
71 physical attributes with suitability values.

72 A wide variety of biological models have been developed over the years to relate
73 physical attributes with habitat suitability values for various life stages of valued
74 salmonid species (Ahmadi-Nedushan et al. 2006; Dunbar et al. 2012). The most

75 common approach uses habitat suitability criteria (HSC), typically as species-specific
76 univariate or multivariate selection functions based on how frequently specific values of
77 each physical attribute are occupied (Dunbar et al. 2012, Rosenfeld et al. 2016). Other
78 HSC-based biological models have also been developed using expert-based fuzzy rule
79 sets (Garbe et al. 2016), bioenergetics (Rosenfeld et al. 2016), and Bayesian statistics
80 (Favrot et al. 2018). Alternatively, probabilistic-based biological models can be used in
81 microhabitat suitability modelling to estimate the probability (between 0 and 1) of a
82 salmonid species and life stage occurring at a specific location given one or more
83 physical attributes (Guay et al. 2000; Hatten et al. 2016; Tiffan et al. 2016).
84 Probabilities ≥ 0.5 are typically categorized as microhabitat where the species should be
85 present, while probabilities < 0.5 are categorized as microhabitat where the species
86 should be absent (Geist et al. 2000; Tiffan et al. 2002; Tiffan et al. 2006; Al-Chokhachy
87 and Budy 2007; Tiffan et al. 2016). Alternative presence-absence probability thresholds
88 can also be used (Hatten et al. 2009; Hatten et al. 2016).

89 Regardless of which biological model is used (i.e., HSC, probabilistic, etc.),
90 microhabitat suitability models are often developed at multiple discharges and/or with
91 multiple restoration design alternatives and used for regulatory and management
92 decisions (Ahmadi-Nedushan et al. 2006; Dunbar et al. 2012). Because of their
93 important role in decision making, microhabitat suitability models should be able to
94 accurately and reliably predict where a species is more or less likely to occur with a
95 high degree of statistical confidence when tested against independent observations (i.e.,
96 observations not used to develop the biological model). However, the metrics
97 commonly used to evaluate the accuracy and reliability of these models are often
98 limited by the methods used to develop them.

99 Microhabitat suitability models developed using probabilistic-based biological
100 models have been tested against independent observations for their ability to predict the
101 presence and absence of spawning (Geist et al. 2008; Hatten et al. 2009; Hatten et al.
102 2016) and rearing (Guay et al. 2000; Tiffan et al. 2006; Tiffan et al. 2016; Hellmair et
103 al. 2018) salmonids. Test metrics include Cohen’s kappa, percentages of microhabitat
104 correctly classified as presence and absence, and errors of commission and omission.
105 However, because these test metrics require the microhabitat suitability model to make
106 a categorical prediction (i.e., presence or absence), they cannot be used to evaluate
107 HSC-based microhabitat suitability models commonly used in ecohydraulic modelling
108 worldwide. This is a significant disadvantage that necessitates alternatives.

109 A more generalized set of tests with strict performance criteria exists that can
110 use independent observational data to evaluate the accuracy and reliability of any type
111 of microhabitat suitability model. Two types of tests are recommended that compare
112 observed data with random analogues to establish statistical significance. The first test
113 is used to determine if there is a significant difference between suitability (or
114 probability) values at utilized and non-utilized locations within the study domain. The
115 second test uses bootstrapped electivity indices calculated for binned suitability values
116 to determine if the model is able to predict both preferred and avoided microhabitat
117 conditions (as defined below) with a high degree of statistical confidence. Pasternack et
118 al. (2014) and Kammel et al. (2016) referred to this set of tests and performance criteria
119 as “bioverification” while reserving the term “validation” for the requisite assessment of
120 hydrodynamic model performance. Such bioverification has been performed for
121 spawning *Oncorhynchus tshawytscha* (Pasternack et al. 2014) and *O. mykiss* (Kammel
122 et al. 2016) microhabitat suitability models, but never for models of rearing salmonids.

123 The goal of this study was to further develop and demonstrate how a generalized
124 yet comprehensive bioverification framework could be used to evaluate the accuracy
125 and reliability of four rearing salmonid microhabitat suitability models using the lower
126 Yuba River (LYR) in California, USA as a testbed. Note that this study is not
127 advocating for these particular models or for HSC-based microhabitat suitability
128 modelling over other modelling approaches. Rather, the novelty of this study is the
129 demonstration of a generalized bioverification framework that can be applied to all
130 microhabitat suitability modelling strategies, regardless of the biological model used.
131 The authors propose that globally, models that pass this rigorous bioverification
132 framework ought to be considered accurate and reliable predictors of microhabitat
133 suitability and appropriate for use in habitat management applications worldwide.

134 **Study site**

135 The Yuba River is a tributary of the Sacramento River in northern California that drains
136 3480 km² of the western slopes of the Sierra Nevada (Figure 1). The LYR, defined as
137 the 37-km segment of the river between Englebright Dam and the Feather River
138 confluence, is a regulated gravel-cobble bed river with a high width-to-depth ratio and
139 slight to no entrenchment (Wyrick and Pasternack 2014). The LYR has a long and
140 complex history of human disturbances, including the deposition of millions of tons of
141 mining sediment during the mid- to late-nineteenth century, dredger re-working of the
142 river and its surrounding area, the installation of the 85-m high Englebright Dam in
143 1941, and flow regulation from a suite of hydroelectric generation facilities located
144 throughout the catchment (Gilbert 1917; James 2005). Despite these multiplicative
145 disturbances, the LYR is hydrogeomorphically dynamic and self-sustaining (Wyrick
146 and Pasternack 2015; Pasternack et al. 2018) and includes critical habitat for Central
147 Valley *O. mykiss* and spring-run *O. tshawytscha*, both listed as threatened under the

148 United States Endangered Species Act (US Fish and Wildlife Service 2010; National
149 Marine Fisheries Service 2014).

150 **Methods**

151 There were several key steps in the development and bioverification of microhabitat
152 suitability models for rearing salmonids in the LYR. Depth and velocity HSC functions
153 were developed for two size classes of *O. tshawytscha* and *O. mykiss* using a subset of
154 microhabitat utilization data from the LYR, while a cover HSC function was developed
155 from previous studies and local fisheries biologists' expert judgement. HSC functions
156 were applied to 0.91-m-resolution (3-ft in sponsor-required American customary units)
157 maps of 2014 hydraulic and cover conditions throughout the entire LYR at multiple
158 discharges resulting in a set of microhabitat suitability models for all four species and
159 size classes. Bioverification tests were then performed on each model at a range of
160 discharges to evaluate their ability to predict preferred and avoided microhabitat
161 conditions beyond the 95% confidence level. Finally, bioverified models were used to
162 quantify rearing habitat area throughout the entire LYR at multiple discharges. An
163 overview of the experimental design is shown in Figure 2. All spatial analyses were
164 performed using ArcGIS (ESRI 2016). All data in the study were collected or generated
165 in American customary units consistent with regulatory requirements and then
166 converted to SI units for this article, hence the appearance of some unusual values in SI
167 units (e.g., 0.91 m represents a 3-ft raster cell size). Full details of this study can be
168 found in the technical reports (Moniz and Pasternack 2019a, 2019b).

169 ***Microhabitat data collection***

170 Rearing microhabitat utilization data were collected during snorkel surveys conducted
171 by Pacific States Marine Fisheries Commission in 2012, 2014, and 2015 (Table 1).

172 These dates and the dates of topographic data collection for hydrodynamic modelling
173 (discussed below) are shown in Figure 3 along with hydrographs of the LYR mean daily
174 discharge recorded at the Smartsville (11418000) and Marysville (11421000) USGS
175 stream gages over the same period.

176 Snorkel surveys were conducted during daylight hours at sites along seven
177 previously designated geomorphic reaches of the LYR (Wyrick and Pasternack 2014).
178 Each snorkel site was randomly selected from a set of 122-m-long intervals that were
179 quantitatively representative of the overall composition of morphological units of each
180 of the seven reaches. For example, if a given geomorphic reach as a whole was 40%
181 pool, 25% riffle, 5% backwater, etc., then the snorkel site randomly selected to
182 represent that reach was composed of those same percentages within 10%.

183 At each snorkel site, four 122-m-long transects were surveyed from upstream to
184 downstream. Transects were spaced roughly equidistantly across the river and included
185 any side channels and/or backwaters in a site. The location of each fish observed was
186 recorded using a Trimble GeoXH GPS handheld unit (differentially corrected horizontal
187 accuracy of ~ 0.5-1.25 m), along with the species of the fish and its associated length,
188 estimated within a 20-mm size class (e.g., 10-30 mm, 30-50 mm, etc.). Salmonids > 150
189 mm were not observed in this study. Associated microhabitat data were also collected at
190 each observation location, including water column depth and mean water column
191 velocity. When multiple fish were observed in close proximity (i.e., less than 1 m apart)
192 utilizing similar microhabitat, snorkelers placed a single marker in the approximate
193 centre of the group and recorded the number and size class of each fish in the group.
194 The location and associated microhabitat data for the group were then recorded at the
195 marker. Non-utilized (i.e., absence) microhabitat data were not recorded during the
196 surveys.

197 ***Subsetting microhabitat data***

198 A common procedure in model calibration and validation studies involves dividing
199 available data between the two main phases of work so that the data are independent in
200 each phase yet representative of the total set. A similar approach was used in this study
201 (Figure 4). Specifically, observations of rearing *O. tshawytscha* and *O. mykiss* were
202 each subset into two size classes (i.e., “fry” < 50 mm and “juvenile” 50 - 150 mm).
203 Two-thirds of the observations from the resulting four species and size class subsets
204 were then used to develop depth and velocity HSC functions, while the remaining
205 observations were set aside to use for bioverification. To ensure representative data in
206 both sets, observations for each species and size class were ordered by date observed
207 and every third observation was set aside for bioverification.

208 One final amendment was made to the bioverification dataset. The microhabitat
209 suitability models developed and tested herein were based on physical conditions of the
210 LYR in 2014. Therefore, the observations used for bioverification had to conform to
211 those conditions. However, Weber and Pasternack (2017) reported changes in river
212 topography between 2008 and 2014, with a brief flood of four times bankfull discharge
213 in December 2012 (Figure 3). In contrast, no significant overbank flooding occurred
214 during the snorkel survey period between May 2014 and August 2015, which is also the
215 period in which 2014 physical data were collected. Because of potential differences in
216 microhabitat conditions between 2012 and 2014, snorkel observations from 2012 were
217 excluded from the bioverification dataset.

218 ***HSC development***

219 Four pairs of depth and velocity HSC functions were developed based on the frequency
220 in which specific microhabitat conditions were utilized (i.e., how often specific depths
221 and velocities were utilized). It has been shown that frequency-based HSC functions

222 developed using abundance data (i.e., number of individuals) provide more detailed
223 outcomes than functions using occurrence data (i.e., number of occupied locations) (Lee
224 and Suen 2013). However, it has also been argued that abundance data may not be the
225 best indicator of habitat quality if high densities of subdominant fish are displaced into
226 low-quality habitat by territorial individuals dominating higher-quality habitat (Beecher
227 et al. 2010). To reduce any potential behaviour-based biases in HSC functions
228 developed in this study, the number of fish counted per observation was recalculated as

$$229 \quad \text{adjusted fish count} = 1 + \log (\text{observed fish count}). \quad (1)$$

230 This approach gave value to each observation while preventing observations with
231 relatively large schools of potentially subdominant fish from significantly reshaping the
232 frequency-based HSC functions. The same adjustment was made to observations used
233 for bioverification (discussed below). The number of observation locations, actual fish
234 counts, and adjusted fish counts used for HSC development and bioverification for each
235 species and size class are shown in Table 2.

236 Frequency distributions of microhabitat utilization data were made for each
237 species and size class using the adjusted fish counts. These distributions were
238 discretized using bin size intervals of 0.03 m and m/s for water column depth and mean
239 channel velocity, respectively. Non-parametric tolerance limits at the 90% confidence
240 level were then used to develop the final HSC functions (Somerville 1958, Remington
241 and Schork 1970, Bovee 1986). Integer limits were treated as percentages of the sample
242 size in order to apply them to the non-integer, log-scaled adjusted counts. Lower limits
243 were not used for velocity HSC functions because utilization was heavily skewed
244 towards near-zero velocities. Following the methods outlined in Bovee (1986), final
245 HSC values were calculated as twice the difference of 1 and the percentage (P) of the
246 population estimated to use that microhabitat range, or

247 HSC value = $2 \cdot (1-P)$. (2)

248 HSC values were then connected by piecewise linear functions, resulting in the final
249 frequency-based HSC functions.

250 A single conditional cover HSC function was developed for all four species and
251 size classes (Table 3). The cover type classifications considered in this study were based
252 on availability of 0.91-m-resolution maps for the entire river under 2014 conditions.
253 Data-driven cover HSC functions could not be developed in this study because cover
254 utilization was not recorded at all fish observations during the snorkel surveys. Instead,
255 the HSC value assigned to vegetation was based on previous studies conducted on the
256 river (Yuba County Water Agency 2013), while values for bedrock outcrops, rip-rap,
257 weirs, and bridge piers were based on local fisheries biologists' expert judgement.
258 Because the LYR's substrate is typically composed of cobble and gravel, with enough
259 large cobble and cobble clusters to provide widespread local cover (Jackson et al. 2013),
260 bare substrate was assigned the HSC value used for cobble substrate in previous studies
261 (Yuba County Water Agency 2013).

262 **Physical model development**

263 *Hydrologic data*

264 A mean daily discharge was obtained or calculated for each bioverification observation
265 using the stream gages associated with that observation (USGS gages 11418000,
266 11418500, and 11421000). The mean daily discharge for each observation was then
267 rounded to the nearest $1.42 \text{ m}^3/\text{s}$ ($50 \text{ ft}^3/\text{s}$) so that observations at relatively similar
268 discharges could be pooled together for bioverification. Thorough sensitivity analysis
269 indicated that pooling the data by a common rounded discharge had a minimal effect on
270 the final suitability associated with each bioverification observation.

271 ***Digital elevation model***

272 Airborne LiDAR combining near-infrared and green wavelength instruments captured
273 the entire terrestrial river corridor topography and approximately 85% of the wetted
274 channel's bathymetry. Deeper areas were mapped with multibeam echosounding.
275 Remaining gaps were mapped with single-beam echosounding and real-time kinematic
276 GPS ground surveys. Topographic-bathymetric map production from these data
277 included extensive quality assurance and quality control measures. The final point cloud
278 had resolutions of 13.17, 5.12, and 3.05 pts/m² in bare earth, bathymetric, and vegetated
279 terrain, respectively. Although these point densities supported sub-meter resolution
280 terrain modelling, other factors also influenced the choice of spatial resolution used in
281 this study, such as the GPS accuracy of the microhabitat utilization data and
282 hydrodynamic model structural assumptions (discussed below). After taking these
283 factors into consideration, a 0.91-m-resolution (3-ft) digital elevation model was
284 produced from the point cloud. Full procedural details were included in the
285 supplementary materials of Weber and Pasternack (2017).

286 ***2D hydrodynamic model***

287 For each rounded mean daily discharge (hereafter referred to as "discharge"), a 0.91-m
288 square grid, steady-state, 2D hydrodynamic model was produced of the entire LYR
289 using ArcGIS and TUFLOW GPU software that solves the 2D depth-averaged Navier-
290 Stokes equations (Huxley and Syme 2016; Pasternack and Hopkins 2017). TUFLOW
291 GPU outputs water depth and depth-averaged water velocity rasters for each discharge
292 simulation.

293 This type of 2D hydrodynamic model is time-averaged, and therefore, does not
294 resolve subgrid-scale turbulence. Because of this structural assumption, the finer the
295 resolution of the computational grid, the more likely the model would be to produce

296 errors in time-averaged results. Thus, the 0.91-m grid used in this study balanced the
297 desire to benefit from sub-meter resolution point cloud data (discussed above) with the
298 risk of violating structural assumptions of the hydrodynamic model. Extensive
299 hydrodynamic validation substantiated the final resolution decision, as results found that
300 model performance far exceeded peer-reviewed journal standards. For example, the
301 median unsigned velocity magnitude error from wading observations was 13%, and the
302 coefficient of determination (R^2) between predicted and observed depth, velocity
303 magnitude, and velocity direction was 0.90, 0.85, and 0.96, respectively. A detailed
304 description of model development and validation is beyond the scope of this study but
305 can be found in Hopkins and Pasternack (2018).

306 *Cover type model*

307 Each cover type polygon was rasterized and buffered out by 0.91 m, a distance
308 determined to represent a biologically reasonable escape distance for fry- and juvenile-
309 sized salmonids. Buffered rasters were then combined into a single raster where each
310 cell was classified as the cover type with the highest HSC value present at that location.
311 For example, a cell with vegetation and rip-rap present was classified as vegetation.

312 **Microhabitat suitability model development**

313 By applying the depth, velocity, and cover HSC functions to the respective hydraulic
314 and cover rasters, a set of 0.91-m-resolution univariate depth, velocity, and cover
315 habitat suitability index (HSI) rasters were created at multiple discharges for all four
316 species and size classes. Depth, velocity, and cover HSI maps were combined cell-by-
317 cell using the geometric mean function, resulting in a combined HSI (CHSI) raster of
318 the entire river for each discharge in which bioverification observations were made for
319 each species and size class. The final microhabitat model resolution of 0.91 m balanced

320 trade-offs between the GPS accuracy of the microhabitat utilization data, digital
321 elevation model resolution, and hydrodynamic model structural assumptions. This
322 approximately 1-m-resolution falls within the range used in other rearing salmonid
323 microhabitat suitability models (Guay et al. 2000; Tiffan et al. 2002; Harrison et al.
324 2011; Gard 2014; Benjanker et al. 2015; Tiffan et al. 2016).

325 **Bioverification**

326 Polygon shapefiles were created at all seven snorkel sites to serve as boundaries for
327 bioverification. At each site, cross-sectional boundaries were manually created
328 perpendicular to the channel at the most upstream and downstream bioverification
329 observations. Therefore, each site boundary was approximately 122-m long, as per
330 snorkel survey protocol. The width of each boundary was the wetted width of the site,
331 and therefore, varied with channel geometry and discharge.

332 ***Mann-Whitney U tests***

333 The Mann-Whitney *U* test is a non-parametric statistical test used to compare the
334 distributions of two independent samples using rank sums, specifically by testing
335 whether one distribution is stochastically greater than the other (Mann and Whitney
336 1947). In this study, the test was used to determine the statistical difference between
337 CHSI values at utilized and non-utilized locations within the river for each species and
338 size class. This simple test has been used to evaluate the performance of other
339 microhabitat suitability models (Gard 2006, 2009, 2014; US Fish and Wildlife Service
340 2010, 2013; Pasternack et al. 2014; Benjanker et al. 2016; Kammel et al. 2016).

341 In this study, a two-tailed Mann-Whitney *U* test was conducted for each
342 microhabitat suitability model and evaluated for statistical differences above the 95%
343 confidence level. A dataset of random points was generated for each species and size

344 class to represent non-utilized observations. The same number of non-utilized points
345 were generated at each site and discharge as in the observed bioverification dataset for
346 each species and size class. Random points were generated within the site boundaries
347 described above. Values were extracted from the appropriate CHSI rasters at utilized
348 and non-utilized point locations, compiled into datasets, and then Mann-Whitney U tests
349 were performed. A p value < 0.05 indicated that the two datasets were statistically
350 different with a 95% confidence level.

351 For a microhabitat suitability model to pass the Mann-Whitney U bioverification
352 test, two performance criteria had to be met. First, CHSI values at utilized and non-
353 utilized locations had to be statistically different according to the Mann-Whitney U test.
354 Second, the median CHSI value at utilized locations had to be higher than the median
355 value at non-utilized locations. These two criteria would be the expected outcome if fish
356 were utilizing microhabitat modelled as having high suitability values over random
357 locations within the same domain. If a model met these criteria, it was then subjected to
358 more rigorous testing, as discussed in detail below.

359 *Forage ratio test*

360 The forage ratio (FR) was originally developed to quantify an organism's preference or
361 avoidance for specific types of prey items (Hess and Swartz 1940; Ivlev 1961), but has
362 also been used more broadly as an index for selection behaviour, including habitat type
363 and quality selection (Williams and Marshall 1938; Johnson 1980; Yuba County Water
364 Agency 2013; Pasternack et al. 2014; Kammel et al. 2016). In general, an FR value can
365 be defined as the ratio of the percent of some resource that is utilized by an organism to
366 the percent of that resource that is available to the organism. In theory, an FR value = 1
367 indicates a resource is neither preferred nor avoided and selection behaviour is
368 indistinguishable from random. In contrast, $FR > 1$ indicates preference for that

369 resource, while $FR < 1$ indicates avoidance. The further an FR value is from one, the
370 more that resource is preferred or avoided. Although several other electivity indices
371 exist with various theoretical trade-offs and could be used in this bioverification
372 framework with equal efficacy, the FR value represents a simple and easy-to-understand
373 metric of preference and avoidance and has been found to be highly suitable for
374 bioverification (Pasternack et al. 2014; Kammel et al. 2016).

375 In this study, FR values were used to determine if microhabitat suitability
376 models were able to accurately predict where preferred and avoided habitat conditions
377 occurred according to CHSI values. To do this, CHSI values were binned into “habitat
378 quality classes”. Past studies have grouped habitat suitability values together using a
379 variety of arbitrarily chosen even (Guay et al. 2000; Hatten et al. 2009; Benjanker et al.
380 2015; Kammel et al. 2016) and uneven (Leclerc et al. 1996; Mäki-Petäys et al. 2002;
381 Harrison et al. 2011) binning intervals. In this study, CHSI values were binned into even
382 intervals of 0.25 (i.e., 0.00-0.25, 0.25-0.50, etc.). FR values were then calculated as the
383 ratio of percent observations to percent available area for each habitat quality class, as
384 detailed below.

385 Bioverification observations were separated into groups based on the snorkel
386 site and discharge at which they were observed. This was done because of the
387 variability in the percentage of area of each habitat quality class across sites and
388 discharges. Observations that occurred at the same site and rounded discharge but on
389 different dates were pooled together. This way, when an observation was made, only the
390 microhabitat within the area that the snorkelers surveyed was considered available to
391 the fish or group of fish observed at that site and discharge. This was determined to be
392 the most accurate representation of the percentages of habitat quality classes that were
393 actually available to each observed fish at a given site and discharge, as oppose to

394 considering the percentages throughout the entire river segment or at sites not surveyed
395 at specific discharges. In accordance with restrictions made in Kammel et al. (2016),
396 bioverification observations located in habitat quality classes that were < 1% of the total
397 available area of a particular site and discharge were excluded from FR analysis.
398 However, no such observations were made in this study.

399 Using adjusted fish counts and site-and-discharge-specific microhabitat
400 availability, an FR value was calculated for each habitat quality class at each site and
401 discharge for all four species and size class models using the equation

$$402 \quad FR_{i,j,k} = \frac{\left(\frac{U_{i,j,k}}{U_{i,k}}\right)}{\left(\frac{A_{i,j,k}}{A_{i,k}}\right)} \quad (3)$$

403 where i was an index defining the species and size class of interest, j was an index for
404 each unique habitat quality class, and k was an index for each site and discharge
405 combination where the species and size class of interest was observed. The numerator
406 term represented the percentage of fish that utilized a habitat quality class at a specific
407 site and discharge using the adjusted fish counts. The denominator term represented the
408 percentage of area of a habitat quality class available at a specific site and discharge.

409 At this step in the analysis, a series of FR values had been calculated for each
410 habitat quality class for all four species and size class models. Each series of FR values
411 was associated with the number of different sites and discharges in which that species
412 and size class was observed. From these series, a single FR value was calculated across
413 sites and discharges for each habitat quality class for each species and size class model
414 using a weighted average. Weights were based on the number of adjusted fish counts at
415 each site and discharge. This was done by computing the weighted-average FR value
416 for each habitat quality class as

417
$$FR_{i,j} = \sum_k^n \left[FR_{i,j,k} \left(\frac{U_{i,k}}{U_i} \right) \right] \quad (4)$$

418 where i, j , and k were the same indices as Equation 3. The fractional term in this
419 equation represented the percent of adjusted fish counts at each site and discharge and
420 was used as the weighting factor when computing the average FR value for each habitat
421 quality class.

422 ***Statistical bootstrapping***

423 As mentioned above, an FR value = 1 indicates that a habitat quality class is neither
424 preferred nor avoided and that selection behaviour is indistinguishable from random.
425 However, the likelihood that an FR value can ever be exactly one is very low. Fewer
426 observations within a dataset can increase the likelihood of random behaviour appearing
427 as actual selection behaviour (i.e., having an FR value slightly greater or slightly less
428 than one). Furthermore, in this study, habitat quality classes with higher suitability
429 values tended to have a smaller percent availability than classes with lower suitability
430 values. These smaller percent availabilities further decreased the likelihood that an
431 average FR value could be exactly one even if the habitat quality classes were being
432 utilized by random chance alone. Therefore, it was necessary to determine with 95%
433 statistical confidence the thresholds above or below one that an average FR value had to
434 be for that habitat quality class to be considered preferred or avoided habitat rather than
435 randomly selected.

436 Thresholds were calculated using statistical bootstrapping, a resampling method
437 that assigns a measure of accuracy to a sample estimate (Efron and Tibshirani 1993).
438 Bootstrapping can be used to determine the confidence intervals of ecological indices
439 (Dixon 2001), including FR values (Kammel et al. 2016). To do this, 20 datasets of
440 randomly generated points were created for each species and size class with the same

441 number of random observations per site and discharge as the observed bioverification
442 dataset. Because observations were scaled logarithmically when computing average FR
443 values, the randomly generated points were randomly assigned the same log-scaled
444 adjusted counts as the observed datasets. For example, if there were five actual
445 observations at a given site and discharge, each with a log-scaled adjusted fish count,
446 the five randomly generated observations at that site and discharge would be randomly
447 assigned one of those five observed adjusted counts, without replacement. This method
448 ensured that the randomly generated observations would produce an average
449 bootstrapped FR value with the same number of terms and the same weighting per site
450 and discharge as the average FR value calculated using the observed data. Therefore,
451 the only difference between the average FR values using the randomly generated points
452 and the actual observations was the spatial randomness.

453 From the 20 sets of FR values calculated using the randomly generated points, it
454 was possible to calculate a 95% confidence interval for each habitat quality class for
455 each species and size class model using a standard deviation, or σ . An upper confidence
456 threshold, or “preference threshold”, was calculated for each habitat quality class as $1 +$
457 2σ , where 1 was the theoretical threshold between preferred and avoided habitat and σ
458 was the standard deviation for that habitat quality class calculated from the 20
459 bootstrapped FR values. Likewise, the lower confidence threshold, or “avoidance
460 threshold”, was calculated for each class as $1 - 2\sigma$.

461 Using the preference and avoidance threshold values from the bootstrapping
462 analysis, the amount by which each observed FR value was above or below the
463 threshold for each habitat quality class was calculated. This final metric will hereafter
464 be referred to as the “FR residual” (i.e., the non-random signal above random chance
465 alone). Habitat quality classes with an observed FR value between the preference and

466 avoidance thresholds (i.e., habitat that was indistinguishable from random selection
467 behaviour) were assigned an FR residual of 0. If the observed FR value was above the
468 preference threshold for that habitat quality class, then the FR residual was calculated as
469 the difference between the observed FR value and the preference threshold. Similarly, if
470 the observed FR value was below the avoidance threshold for that habitat quality class,
471 then the FR residual was calculated as the difference between the observed FR value
472 and the avoidance threshold. The result of these computations were FR residuals centred
473 at 0, where positive values indicated preference and negative values indicated
474 avoidance. Using the FR residual as a final metric for analysing bioverification results
475 removes the statistical uncertainty that may arise from relatively small datasets, habitat
476 quality classes with small percent availability, and potentially other ecological factors
477 not explicitly considered in the microhabitat suitability models themselves.

478 For the four microhabitat models to pass the forage ratio test and be considered
479 bioverified, two performance criteria had to be met. First, one or more habitat quality
480 classes had to be considered preferred and one or more had to be avoided, as indicated
481 by FR residuals. Second, FR residuals had to monotonically increase with increasing
482 CHSI values across habitat quality classes. These criteria insured that bioverified
483 models were able to predict both preferred and avoided habitat and that FR residuals
484 followed a logical order. Models that met these criteria were considered bioverified and
485 successful predictors of microhabitat suitability in the LYR.

486 ***Habitat area-discharge relationship***

487 Bioverified microhabitat suitability models were used to quantify the percentage of area
488 of each habitat quality class throughout the entire LYR at multiple discharges.
489 Percentages were calculated at each discharge in which bioverification observations
490 were made for each species and size class. To normalize the percentages across

491 discharges, the area of each habitat quality class was divided by the area of the wetted
492 channel at the highest discharge in which a bioverification observation was made for
493 that species and size class. The percentage of unwetted area was also calculated for each
494 discharge relative to the area of the wetted channel at the highest discharge. For
495 example, the area for each *O. tshawytscha* fry habitat quality class was calculated
496 throughout the entire river at 14.16 m³/s and then divided by the area of the wetted
497 channel at 32.56 m³/s. The percentage of unwetted area was also calculated at 14.16
498 m³/s as the difference between the area of wetted channel at 32.56 and 14.16 m³/s
499 divided by the area of wetted channel at 32.56 m³/s. By using this method, percentages
500 of area for each habitat quality class were relative to the same area for each species and
501 size class and could therefore be compared across discharges.

502 **Results**

503 *HSC development*

504 *O. tshawytscha* and *O. mykiss* juveniles utilized deeper and faster microhabitat
505 compared to the fry size class of both species (Table 4). Depth and velocity HSC
506 functions reflected these tendencies with peak suitability values extending towards
507 slightly deeper and faster water for juveniles compared to fry (Figure 5). As expected,
508 ranges of peak suitability encompassed the mean, median, and mode depth and velocity
509 values utilized by all four species and size classes. Depth and velocity HSC functions
510 exhibited similar shapes across species and size classes except for *O. mykiss* fry, which
511 were not observed in depths greater than 0.93 m in the HSC or bioverification datasets.

512 *Mann-Whitney U test results*

513 Mann-Whitney *U* test results showed statistically significant differences between CHSI
514 values at randomly generated, non-utilized locations and locations utilized by all four

515 species and size classes (Table 5; Figure 6). Although all four microhabitat suitability
516 models met performance criteria necessary to pass the Mann-Whitney U bioverification
517 test, there were noticeable differences in distributions of utilized and non-utilized CHSI
518 values between species and size classes. For example, the interquartile range of utilized
519 and non-utilized CHSI values for both *O. tshawytscha* size classes overlapped, while
520 there was no overlap for either *O. mykiss* size class (Figure 6). For *O. mykiss* fry,
521 relatively narrow depth and velocity HSC functions (Figure 5) caused a significant
522 proportion of the modelled channel to have a suitability value of zero. Most of the
523 non-utilized locations were then randomly generated where microhabitat suitability was
524 zero, resulting in an interquartile range of zero. The lack of overlap in utilized and non-
525 utilized values for *O. mykiss* juveniles is less straightforward and may be the result of
526 lower intraspecific competition for highly suitable microhabitat compared to the more
527 abundant *O. tshawytscha* size classes (Table 2).

528 ***Forage ratio and bootstrapping results***

529 Statistical bootstrapping showed variability in preference and avoidance thresholds
530 across habitat quality classes and the four species and size classes (Table 6). In general,
531 the standard deviations and resulting threshold ranges increased with increasing habitat
532 quality for all species and size class models. This increase was likely because habitat
533 quality classes with higher CHSI values made up smaller percentages of the total area
534 within the channel across sites and discharges compared to classes with lower values.
535 With smaller areas, there were lower probabilities of randomly generated points falling
536 within those classes, causing lower than average FR values. However, because the areas
537 were smaller, when randomly generated points did fall within those habitat quality
538 classes, FR values were above average. A combination of high and low FR values when
539 randomly generated points did and did not fall within classes with relatively smaller

540 areas resulted in larger standard deviations and resulting thresholds for those classes.
541 Larger standard deviations were also due in part to smaller datasets. Datasets for both
542 *O. tshawytscha* size classes generally had more observations and smaller standard
543 deviations than the *O. mykiss* size classes.

544 There was a similar monotonic increase in FR residuals with increasing habitat
545 quality classes across all species and size class models (Table 6, Figure 7). All four
546 species and size classes avoided the lowest class and preferred the highest. However, all
547 four species and size classes did not share the same preference and avoidance for the
548 0.25-0.50 and 0.50-0.75 classes. For example, *O. mykiss* fry strongly preferred CHSI
549 values in the 0.50-0.75 class, while *O. mykiss* juveniles neither preferred nor avoided
550 them. Overall, all four microhabitat suitability models met the two performance criteria
551 necessary to pass the FR bioverification test and were therefore considered bioverified
552 and successful models of microhabitat suitability in the LYR.

553 Four example sites were chosen to illustrate the performance of each species and
554 size class microhabitat suitability model (Figure 8). At each example site, a majority of
555 observations were located along the banks and in the 0.75-1.00 habitat quality class,
556 while no observations were made midchannel or in the 0.00-0.25 class. These examples
557 highlight the ability of all four models to make relatively accurate and detailed
558 predictions of microhabitat preference and avoidance.

559 ***Habitat area-discharge relationship***

560 The percentage of area of each habitat quality class varied across species, size class, and
561 discharge (Figure 9). The 0.75-1.00 class made up the smallest percentage of area for
562 each species, size class, and discharge and only decreased slightly with increasing
563 discharge. For fry size classes of both species, the percentage of area for the 0.50-0.75
564 and 0.25-0.50 classes decreased with increasing discharge, while only the 0.50-0.75

565 classes decreased with increasing discharge for juveniles. The 0.00-0.25 class increased
566 with increasing discharge for all four species and size classes, but at a slightly higher
567 rate for fry than for juveniles.

568 **Discussion**

569 *What constitutes bioverification?*

570 While not considered bioverification as defined in this article, biological models used to
571 estimate salmonid habitat quality have been evaluated and compared many different
572 ways since the 1970s (Ahmadi-Nedushan et al. 2006; Dunbar et al. 2012). Regression
573 analysis has been used to evaluate the correlation between suitability values estimated
574 by HSC functions and salmonid biomass or density (Wesche et al. 1987; Beard and
575 Carline 1991; Beecher et al. 2002), while chi-squared tests have been used to validate
576 the transferability of HSC functions between rivers (Thomas and Bovee 1993, Mäki-
577 Petäys et al. 2002; Guay et al. 2003). For probabilistic-based biological models,
578 Akaike's information criterion, pseudo-R² values, and the Hosmer-Lemeshow statistic
579 have been used to evaluate and compare the goodness-of-fit of different models, while
580 metrics of selectivity, sensitivity, and errors of omission and commission are commonly
581 used to test classification accuracy (Tiffan et al. 2006; Hatten et al. 2009; Hatten et al.
582 2016; Tiffan et al. 2016; Hellmair et al. 2018).

583 Compared to the large number of biological models developed and evaluated for
584 salmonids and other aquatic organisms, there have been relatively few studies that have
585 tested the ability of microhabitat suitability models to accurately and reliably predict
586 where these species are more or less likely to occur using independent observational
587 data. Although probabilistic-based microhabitat suitability models have been tested
588 against independent observations of spawning (Geist et al. 2008; Hatten et al. 2009;

589 Hatten et al. 2016) and rearing (Guay et al. 2000; Tiffan et al. 2006; Tiffan et al. 2016;
590 Hellmair et al. 2018) salmonids, the metrics used in these tests require a categorical
591 prediction of habitat suitability (i.e., presence or absence). These metrics are therefore
592 unable to evaluate the wide variety non-probabilistic predictive models commonly used
593 in ecohydraulic modelling worldwide.

594 Although microhabitat suitability models have become a relatively common tool
595 used in ecohydraulics, there remains no consensus regarding which tests should be used
596 and what degree of performance should be required for a model to be accepted for basic
597 science and societal applications. Building on previous studies and preceding work by
598 Kammel et al. (2016), this study proposes a generalized yet comprehensive and
599 transparent framework for evaluating predictions made by any type of microhabitat
600 suitability model with a high degree of statistical confidence and clear performance
601 criteria. Two types of tests are recommended that compare observed data with random
602 analogues to establish statistical significance. This testing framework is on par with
603 hydrodynamic model validation and constitutes ecohydraulic model bioverification as
604 defined in this article. By meeting the performance criteria of these tests, the models
605 developed herein showed statistically significant differences between suitability values
606 at utilized and non-utilized locations in the LYR and predicted both preferred and
607 avoided microhabitat conditions with statistical confidence.

608 ***Habitat quality class binning***

609 A key analytical step in this study was binning CHSI values into habitat quality classes
610 for forage ratio and bootstrapping analyses. Although binning suitability values is a
611 traditional and straightforward strategy used in ecohydraulic modelling (Leclerc et al.
612 1996; Guay et al. 2000; Mäki-Petäys et al. 2002; Hatten et al. 2009; Harrison et al.
613 2011; Benjanker et al. 2015; Kammel et al. 2016), it is typically done using arbitrarily

614 chosen binning intervals. With the bioverification framework used in this study,
615 however, it is possible to substantiate the veracity of binning schemes by evaluating
616 which bins are avoided, randomly selected, and preferred. Further, although outside the
617 scope of this study, forage ratio and bootstrapping analyses allow simple three-class
618 binning schemes with optimal bin ranges for avoided, randomly selected, and preferred
619 habitat quality classes. Specifically, a computer program could be developed that
620 optimizes all three classes by incrementally shifting the bin ranges of each class and
621 then calculating the associated FR residuals until a specific optimized outcome was
622 reached.

623 Another important consideration of habitat quality class binning is the value of a
624 bioverified two-class scheme with preferred habitat as one class and avoided and
625 randomly selected habitat as the other class. With this binning scheme, the actual area
626 of preferred habitat can be analysed across discharges and/or with alternative restoration
627 designs rather than the commonly used but highly criticized weighted usable area
628 (WUA) habitat index (Railsback 2016). For these reasons, the forage ratio and
629 bootstrapping approach presented herein are a significant analytical development with
630 the potential to enhance ecohydraulic modelling and habitat analyses in diverse
631 applications.

632 *Assessing study assumptions*

633 An assumption made in this study was that depth and velocity suitability values for
634 rearing salmonids remain constant as discharge changes. For example, for each species
635 and size class, the same set of frequency-based HSC functions were applied to depth
636 and velocity raster outputs hydrodynamically modelled from 14.16 to 42.48 m³/s.
637 Additionally, weighted average FR values were calculated across this same range of
638 discharges. In support of this assumption, several studies have observed no statistically

639 significant difference between the depths and velocities utilized by rearing salmonids at
640 varying discharges (Heggens 1988; Shirvell 1994; Beecher et al. 1995; Robertson et al.
641 2004). These observations suggest that rearing salmonids change locations within the
642 channel to remain at suitable depths and velocities as discharge changes. In other
643 studies, however, adult (Pert and Erman 1994) and rearing (Vehanen et al. 2000, Holm
644 et al. 2001) salmonids were observed utilizing deeper and faster (i.e., less suitable)
645 microhabitat conditions as discharge rapidly changed. These conflicting results suggest
646 that other factors may be responsible for the observed changes in utilized depths and
647 velocities as discharge changes. For example, availability of suitable depths and
648 velocity conditions may decrease more rapidly at some study sites compared to others
649 as discharge increases, functionally forcing fish to utilize deeper and faster water. Yet
650 this pattern was not observed in the LYR during this study. Rather, suitable depth and
651 velocity conditions were abundant across all sites and discharges according to validated
652 2D hydrodynamic model outputs.

653 There are also other factors not considered in the microhabitat suitability models
654 evaluated in this study. For example, water temperature can affect salmonid mortality
655 (Richter and Kolmes, 2005), growth (Marine and Cech 2004), movement (Baker et al.
656 1995), and diel activity (Fraser et al. 1995). Although water temperatures in the LYR
657 are unlikely to reach levels high enough to cause mortality to rearing salmonids,
658 temperatures that maximize growth and swimming ability are likely a major component
659 of temporal microhabitat selection (Hillman et al. 1987; Taylor 1988; Allen 2000).
660 Similarly, food availability (Dill et al. 1981), competition for preferred habitat between
661 and among fish species (Everest and Chapman 1972; Grant et al. 1990), and predation
662 (Bugert and Bjornn 1991; Tiffan et al. 2016) can also affect microhabitat quality and
663 availability for rearing salmonids. Despite these considerations, the microhabitat

664 suitability models evaluated in this study passed several steps of a rigorous
665 bioverification framework and demonstrated an ability to accurately and reliably predict
666 preferred and avoided rearing salmonid habitat in the LYR.

667 **Conclusions**

668 In this study, four sets of frequency-based, data-driven depth and velocity HSC
669 functions were developed for rearing salmonids in the LYR. These sets of HSC
670 functions, along with an expert-based cover HSC function were applied to spatially
671 explicit, 0.91-m-resolution maps of physical habitat conditions throughout the 37-km
672 long river, resulting in four microhabitat suitability models. The models were then
673 bioverified using a general yet comprehensive framework with transparent uncertainty
674 analysis and performance criteria. The rearing salmonid microhabitat models developed
675 herein were not only able to show statistically significant differences between suitability
676 values at utilized and non-utilized locations for all four species and size classes, but
677 were also able to predict both preferred and avoided microhabitat conditions with
678 statistical confidence through forage ratio and bootstrapping analyses. Bioverified 2D
679 microhabitat suitability models allow for a more detailed and spatially explicit
680 representation of discharge-dependent habitat conditions than traditional transect-based
681 and 1D microhabitat models (e.g., PHABSIM). As a result, they can provide more
682 accurate and spatially interpretable predictions of preferred habitat area for regulatory
683 and management decisions, including instream flow assessments and habitat restoration
684 efforts. Although demonstrated as a method for evaluating salmonid microhabitat
685 suitability models, this bioverification framework can be applied to any spatially
686 explicit habitat suitability model, regardless of species, life stage, or habitat type.

687 **Acknowledgements**

688 The authors would like to thank Casey Campos, Ryan Greathouse, Derek Givens, Leslie
689 Alber, Kyle Thompson, Byron Mache, Matthew Weber, Chelsea Hopkins, and Paulo
690 Silva for their assistance in collecting and processing data used in this study as well as
691 Geoff Rabone, Sebastian Schwindt, Sean Luis, and several anonymous reviewers for
692 their feedback on previous drafts of this manuscript.

693 **Funding**

694 Primary support for this study was provided by the Yuba Water Agency [award number
695 201016094] and as in-kind aid from the Yuba Accord River Management Team. This
696 project was also supported by the USDA National Institute of Food and Agriculture,
697 Hatch [project number CA-D-LAW-7034-H] and scholarships from the Fly Fishers of
698 Davis, California Fly Fishers Unlimited, and Diablo Valley Fly Fishing Club.

699 **References**

- 700 Ahmadi-Nedushan B, St-Hilaire A, Bérubé M, Robichaud É, Thiémonge N, Bobée B.
701 2006. A review of statistical methods for the evaluation of aquatic habitat
702 suitability for instream flow assessment. *River Res Appl.* 22(5):503-523.
- 703 Al-Chokhachy R, Budy P. 2007. Summer microhabitat use of fluvial Bull Trout in
704 eastern Oregon streams. *North Am J Fish Manage.* 27(4):1068-1081.
- 705 Allen MA. 2000. Seasonal microhabitat use by juvenile spring Chinook salmon in the
706 Yakima River Basin, Washington. *Rivers.* 7:314-332.
- 707 Anim DO, Fletcher TD, Vietz GJ, Pasternack GB, Burns MJ. Restoring in-stream
708 habitat in urban catchments: Modify flow or the channel? *Ecohydrology.* 12:1-
709 16.
- 710 Arif MSM, Gülch E, Tuhtan JA, Thumser P, Haas C. 2017. An investigation of image
711 processing techniques for substrate classification based on dominant grain size
712 using RGB images from UAV. *Int J Remote Sens.* 38(8-10):2639-2661.
- 713 Baker PF, Ligon, FK, Speed TP. 1995. Estimating the influence of temperature on the
714 survival of Chinook salmon smolts (*Oncorhynchus tshawytscha*) migrating

715 through the Sacramento-San Joaquin River Delta of California. *Can J Fish*
716 *Aquat Sci.* 52(4):855-863.

717 Beard TD, Carline RF. 1991. Influence of spawning and other stream habitat features on
718 spatial variability of wild brown trout. *Trans Am Fish Soc.* 120(6):711-711.

719 Beecher HA, Caldwell BA, DeMond SB. 2002. Evaluation of depth and velocity
720 preferences of juvenile coho salmon in Washington streams. *North Am J Fish*
721 *Manage.* 22(3):785-795.

722 Beecher HA, Caldwell BA, DeMond SB, Seiler D, Boessow SN. 2010. An empirical
723 assessment of PHABSIM using longterm monitoring of coho salmon smolt
724 production in Bingham Creek, Washington. *North Am J Fish Manage.*
725 30(6):1529-1543.

726 Beecher HA, Carleton JP, Johnson TH. 1995. Notes: utility of depth and velocity
727 preferences for predicting steelhead parr distribution at different flows. *Trans*
728 *Am Fish Soc.* 124(6):935-938.

729 Benjanker R, Tonina D, Marzadri A, McKean J, Issak DJ. 2016. Effects of habitat
730 quality and ambient hyporheic flows on salmon spawning site selection. *J.*
731 *Geophys. Res. Biogeosci.* 121:1221-1435.

732 Benjanker R, Tonina D, McKean J. 2015. One-dimensional and two-dimensional
733 hydrodynamic modeling derived flow properties: impacts on aquatic habitat
734 quality predictions. *Earth Surf Processes Landforms.* 40:340-356.

735 Bovee KD. 1986. Development and evaluation of habitat suitability criteria for use in
736 the instream flow incremental methodology. Washington (DC): US Fish and
737 Wildlife Service. Instream Flow Information Paper #21 FWS/OBS-86/7.

738 Bugert RM, Bjornn TC. 1991. Habitat use by steelhead and coho salmon and their
739 responses to predators and cover in laboratory streams. *Trans Am Fish Soc.*
740 120(4):486-493.

741 Dill LM, Ydenberg RC, Fraser AHG. 1981. Food abundance and territory size in
742 juvenile coho salmon (*Oncorhynchus kisutch*). *Can J Zool.* 59(9):1801-1809.

743 Dixon PM. 2001. The bootstrap and the jackknife: describing the precision of ecological
744 indices. In: Scheiner SM, Gurevitch J, editors. *Design and analysis of ecological*
745 *experiments.* New York (NY): Oxford University Press. p. 267-288.

746 Dunbar MJ, Alfredsen K, Harby A. 2012. Hydraulic-habitat modelling for setting
747 environmental river flow needs for salmonids. *Fisheries Manag Ecol.* 19(6):500-
748 517.

749 Efron B, Tibshirani R. 1993. An Introduction to the Bootstrap. Boca Raton (FL):
750 Chapman & Hall/CRC.

751 ESRI. 2016. ArcGIS Desktop: Release 10.5. Redlands (CA): Environmental Systems
752 Research Institute.

753 Everest FH, Chapman DW. 1972. Habitat selection and spatial interaction by juvenile
754 Chinook salmon and steelhead trout in two Idaho streams. J Fish Res Board
755 Can. 29(1):91-100.

756 Favrot SD, Jonasson BC, Peterson JT. 2018. Fall and winter microhabitat use and
757 suitability for spring Chinook salmon parr in a U.S. Pacific Northwest River.
758 Trans Am Fish Soc. 147(1):151-170.

759 Fraser NHC, Metcalfe NB, Heggenes J, Thorpe JE. 1995. Low summer temperatures
760 cause juvenile Atlantic salmon to become nocturnal. Can J Zool. 73(3):446-451.

761 Garbe J, Beevers L, Pender G. 2016. The interaction of low flow conditions and
762 spawning brown trout (*Salmo trutta*) habitat availability. Ecol Eng. 88:53-63.

763 Gard M. 2006. Modeling changes in salmon spawning and rearing habitat associated
764 with river channel restoration. Int J River Basin Manage. 4(3):201-211.

765 Gard M. 2009. Comparison of spawning habitat predictions of PHABSIM and River2D
766 models. Int J River Basin Manage. 7(1):55-71.

767 Gard M. 2014. Modelling changes in salmon habitat associated with river channel
768 restoration and flow-induced channel alternations. River Res Appl. 30(1):40-
769 44.

770 Geist DR, Jones J, Murray CJ, Dauble D. 2000. Suitability criteria analysed at the
771 spatial scale of red clusters improved estimates of fall chinook salmon
772 (*Oncorhynchus tshawytscha*) spawning habitat use in the Hanford Reach,
773 Columbia River. Can J Fish Aquat Sci. 57(8):1636-1646.

774 Geist DR, Murray CJ, Hanrahan TP, Xie Y. 2008. A model of the effects of flow
775 fluctuation on fall Chinook salmon spawning habitat availability in the
776 Columbia River. North Am J Fish Manage. 28(6):1894-1910.

777 Gibson SA, Pasternack GB. 2015. Selecting between one-dimensional and two-
778 dimensional hydrodynamic models for ecohydraulic analysis. River Res Appl.
779 32(6):1365-1381.

780 Gilbert GK. 1917. Hydraulic-mining debris in the Sierra Nevada. Washington (DC): US
781 Geological Survey.

782 Grant JWA, Kramer DL. 1990. Territory size as a predictor of the upper limit to
783 population density of juvenile salmonids in streams. *Can J Fish Aquat Sci.*
784 47(9):1724-1737.

785 Guay JC, Boisclair D, Leclerc M, Lapointe M, Legendre P. 2003. Assessment of the
786 transferability of biological habitat models for Atlantic salmon parr (*Salmo*
787 *salar*). *Can J Fish Aquat Sci.* 60(11):1398-1408.

788 Guay JC, Boisclair D, Rioux D, Leclerc M, Lapointe M, Legendre P. 2000.
789 Development and validation of numerical habitat models for juveniles of
790 Atlantic salmon (*Salmo salar*). *Can J Fish Aquat Sci.* 57(10):2065-2075.

791 Guse B, Kail J, Radinger J, Schröder M, Kiesel J, Hering D, Wolter C, Fohrer N. 2015.
792 Eco-hydrologic model cascades: Simulating land use and climate change
793 impacts on hydrology, hydraulics and habitats for fish and macroinvertebrates.
794 *Sci Total Environ.* 533:542-556.

795 Harrison LR, Legleiter CJ, Wydzga MA, Dunne T. 2011. Channel dynamics and habitat
796 development in a meandering, gravel bed river. *Water Resour Res.* 47:1-21.

797 Hatten JR, Batt TR, Skalicky JJ, Engle R, Barton GJ, RL Fosness, Warren J. 2016.
798 Effects of dam removal on Tule fall Chinook salmon spawning habitat in the
799 White Salmon River, Washington. *River Res Applic.* 32(7):1481-1492.

800 Hatten JR, Tiffan KF, Anglin DR, Haeseker SL, Skalicky JJ, Schaller H. 2009. A spatial
801 model to assess the effects of hydropower operations on Columbia River fall
802 Chinook salmon spawning habitat. *North Am J Fish Manage.* 29(5):1379-1405.

803 Heggenes J. 1988. Effect of short-term flow fluctuations on displacement of, and habitat
804 use by brown trout in a small stream. *Trans Am Fish Soc.* 117(4):336-344.

805 Hellmair M, Peterson M, Mulvey B, Young K, Montgomery J, Fuller A. 2018. Physical
806 characteristics influencing nearshore habitat use by juvenile Chinook salmon in
807 the Sacramento River, California. *North Am J Fish Manage.* 38(4):959-970.

808 Hess AD, Swartz A. 1940. The forage ratio and its use in determining the food grade of
809 streams. *Trans N Am Wildl Conf.* 5:162-164.

810 Hillman TW, Griffith JS, Platts WS. 1987. Summer and winter habitat selection by
811 juvenile Chinook salmon in a highly sedimented Idaho stream. *Trans Am Fish*
812 *Soc.* 116(2):185-195.

813 Holm CF, Armstrong JD, Gilver DJ. 2001. Investigating a major assumption of
814 predictive instream habitat models: is water velocity preference of juvenile
815 Atlantic salmon independent of discharge? *J Fish Biol.* 59(6):1653-1666.

816 Hopkins CE, Pasternack GB. 2018. Autumn 2014 lower Yuba River TUFLOW GPU
817 2D model description and validation. Davis (CA): University of California at
818 Davis. Prepared for Yuba County Water Agency.

819 Huxley C, Syme B. 2016. TUFLOW GPU – best practice advice for hydrologic and
820 hydraulic model simulations. Paper presented at: Hydrology and Water
821 Resources Symposium, Queenstown, New Zealand.

822 Ivlev VS. 1961. Experimental ecology of the feeding of fishes. New Haven (CT): Yale
823 University Press.

824 Jackson JR, Pasternack GB, Wyrick JR. 2013. Substrate of the lower Yuba River. Davis
825 (CA): University of California at Davis. Prepared for the Yuba Accord River
826 Management Team.

827 James LA, 2005. Sediment from hydraulic mining detained by Englebright Dam and
828 small dams in the Yuba Basin. *Geomorphology*. 71(1-2):202-226.

829 Johnson DH. 1980. The comparison of usage and availability measurements for
830 evaluating resource preference. *Ecology* 61(1):65-71.

831 Kammel LE, Pasternack GB, Massa DA, Bratovich PM. 2016. Near-census
832 ecohydraulics bioverification of *Oncorhynchus mykiss* spawning microhabitat
833 preferences. *J Ecohydraulics*. 1(1-2):62-78.

834 Lallias-Tacon S, Liébault F, Piégay H. 2017. Use of airborne LiDAR and historical
835 aerial photos for characterising the history of braided river floodplain
836 morphology and vegetation responses. *Catena*. 149:742-759.

837 Lamb BL, Sabaton C, Souchon Y. 2004. Use of the instream flow incremental
838 methodology: introduction to the special issue. *Hydroécologie Appliquée* 14:1-
839 7.

840 Lamouroux N, Capra H, Pouilly M. 1998. Predicting habitat suitability for lotic fish:
841 linking statistical hydraulic models with multivariate habitat use models. *Regul*
842 *River*. 14(1):1-11.

843 Leclerc M, Boudreault A, Bechara JA, Corfa G. 1996. Two-dimensional hydrodynamic
844 modeling: a neglected tool in the instream flow incremental methodology. *Trans*
845 *Am Fish Soc*. 124(5):645-662.

846 Lee P, Suen J. 2013. Comparing habitat suitability indices (HSIs) based on abundance
847 and occurrence data. *North Am J Fish Manage*. 33(1):89-96.

848 Mann HB, Whitney DR. 1947. On a test of whether one of two random variables is
849 stochastically larger than the other. *Ann Math Stat*. 18(1):50-60.

850 Mäki-Petäys A, Huusko A, Erkinaro J, Muotka T. 2002. Transferability of habitat
851 suitability criteria of juvenile Atlantic salmon (*Salmo salar*). Can J Fish Aquat
852 Sci. 59(2):218-228.

853 Marine KR, Cech JJ. 2004. Effects of high water temperature on growth, smoltification,
854 and predator avoidance in juvenile Sacramento River Chinook salmon. North
855 Am J Fish Manage. 24(1):198-210.

856 Meybeck M. 2003. Global analysis of river systems: from Earth system controls to
857 Anthropocene syndromes. Philos Trans Roy Soc B. 358(1440):1935-1955.

858 Moniz PJ, Pasternack GB. 2019a. Bioverification of microhabitat suitability models for
859 rearing salmonids in the lower Yuba River. Davis (CA): University of California
860 at Davis. Prepared for Yuba Water Agency.

861 Moniz PJ, Pasternack GB. 2019b. Habitat suitability curves for rearing salmonids in the
862 lower Yuba River. Davis (CA): University of California at Davis. Prepared for
863 Yuba Water Agency.

864 National Marine Fisheries Service. 2014. Recovery plan for the evolutionarily
865 significant units of Sacramento River winter-run Chinook salmon and Central
866 Valley spring-run Chinook salmon and the distinct population segment of
867 California Central Valley steelhead. California Central Valley Area Office. July
868 2014.

869 Pasternack GB, Baig D, Weber MD, Brown RA. 2018. Hierarchically nested river
870 landform sequences. Part 2: Bankfull channel morphodynamics governed by
871 valley nesting structure. Earth Surf Processes Landforms. 43(12):2519-2532.

872 Pasternack GB, Hopkins CE. 2017. Near-census 2D model comparison between SRH-
873 2D and TUFLOW GPU for use in gravel/cobble rivers. Davis (CA): University
874 of California at Davis. Prepared for Yuba County Water Agency.

875 Pasternack GB, Tu D, Wyrick JR. 2014. Chinook adult salmon spawning physical
876 habitat of the lower Yuba River. Final report. Davis (CA): Lower Yuba River
877 Accord Monitoring and Evaluation Program.

878 Pasternack GB, Wang CL, Merz JE. 2004. Application of a 2D hydrodynamic model to
879 design of reach-scale spawning gravel replenishment on the Mokelumne River,
880 California. River Res Appl. 20:205-225.

881 Pert EJ, Erman DC. 1994. Habitat use by adult rainbow trout under moderate artificial
882 fluctuations in flow. Trans Am Fish Soc. 123(6):913-923.

883 Railsback SF. 2016. Why it is time to put PHABSIM out to pasture. Fisheries.
884 41(12):720-725.

885 Remington RD, Schork MA. 1970. Statistics with applications to the biological and
886 health sciences. Englewood Cliffs (NJ): Prentice-Hall.

887 Richter A, Kolmes SA. 2005. Maximum temperature limits for Chinook, coho, chum
888 salmon, and steelhead trout in the Pacific Northwest. Rev Fish Sci. 13(1):23-49.

889 Robertson MJ, Pennell CJ, Scruton DA, Robertson GJ, Brown JA. 2004. Effect of
890 increased flow on the behaviour of Atlantic salmon parr in winter. J Fish Biol.
891 65(4):1070-1079.

892 Rosenfeld J, Beecher H, Ptolemy R. 2016. Developing bioenergetics-based habitat
893 suitability curves for instream flow models. North Am J Fish Manage.
894 36(5):1205-1219.

895 Schwindt S, Pasternack GB, Bratovich PM, Rabone G, Simodynes D. 2019. Hydro-
896 morphological parameters generate lifespan maps for stream restoration
897 management. J Environ Manage. 232:475-489.

898 Shirvell CS. 1994. Effect of changes in streamflow on the microhabitat use and
899 movements of sympatric juvenile coho (*Oncorhynchus kisutch*) and Chinook
900 salmon (*O. tshawytscha*) in a natural stream. Can J Fish Aquat Sci. 51(7):1644-
901 1652.

902 Somerville PN. 1958. Tables for obtaining non-parametric tolerance limits. Ann Math
903 Stat. 29(2):599-601.

904 Taylor EB. 1988. Water temperature and velocity as determinants of microhabitats of
905 juvenile Chinook and coho salmon in a laboratory stream channel. Trans Am
906 Fish Soc. 117(1):22-28.

907 Tharme RE. 2003. A global perspective on environmental flow assessment: emerging
908 trends in the development and application of environmental flow methodologies
909 for rivers. River Res Appl. 19(5-6):397-441.

910 Thomas JA, Bovee KD. 1993. Application and testing of a procedure to evaluate
911 transferability of habitat suitability criteria. Regul River. 8(3):285-294.

912 Tiffan KF, Garland RD, Rondorf DW. 2002. Quantifying flow-dependent changes in
913 subyearling fall Chinook salmon rearing habitat using two-dimensional spatially
914 explicit modeling. North Am J Fish Manage. 22(3):713-726.

915 Tiffan KF, Clark LO, Garland RD, Rondorf DW. 2006. Variables influencing the
916 presence of subyearling fall Chinook salmon in shoreline habitats on the
917 Hanford Reach, Columbia River. *North Am J Fish Manage.* 26(2):351-360.

918 Tiffan KF, Hatten JR, Trachtenbarg DA. 2016. Assessing juvenile salmon rearing
919 habitat and associated predation risk in a lower Snake River reservoir. *River Res*
920 *Appl.* 32(5):1030-1038.

921 US Fish and Wildlife Service. 2010. Flow-habitat relationships for juvenile fall/spring-
922 run Chinook salmon and steelhead/rainbow trout rearing in the Yuba River.
923 Sacramento (CA): US Fish and Wildlife Service.

924 US Fish and Wildlife Service. 2013. Flow-habitat relationships for juvenile spring-run
925 and fall-run Chinook salmon and steelhead/rainbow trout rearing in Clear Creek
926 between Clear Creek Road and the Sacramento River. Sacramento (CA): US
927 Fish and Wildlife Service.

928 Vehanen T, Bjerke PL, Heggenes J, Huusko A, Mäki-Petäys A. 2000. Effect of
929 fluctuating flow and temperature on cover type selection and behaviour by
930 juvenile brown trout in artificial flumes. *J Fish Biol.* 56(4):923-937.

931 Waddle TJ. 2001. PHABSIM for Windows: user's manual and exercises. Fort Collins
932 (CO): US Geological Survey. Open File Report 2001-340.

933 Weber MD, Pasternack GB. 2017. Valley-scale morphology drives differences in fluvial
934 sediment budgets and incision rates during contrasting flow regimes.
935 *Geomorphology.* 288:39-51.

936 Wesche TA, Goertler CM, Hubert WA. 1987. Modified habitat suitability index for
937 brown trout in southeastern Wyoming. *North Am J Fish Manage.* 7(2):232-237.

938 Williams CS, Marshall WH. 1938. Duck nesting studies, Bear River Migratory Bird
939 Refuge, Utah, 1937. *J Wildlife Manage.* 2(2):29-48.

940 Wyrick JR, Pasternack GB. 2014. Geospatial organization of fluvial landforms in a
941 gravel-cobble river: beyond the riffle-pool couplet. *Geomorphology.* 213:48-65.

942 Wyrick JR, Pasternack GB. 2015. Revealing the natural complexity of topographic
943 change processes through repeat surveys and decision-tree classification. *Earth*
944 *Surf Processes Landforms.* 41(6):723-737.

945 Yuba County Water Agency. 2013. Technical memorandum 7-10: instream flow
946 downstream of Englebright Dam. Marysville (CA): Yuba River Development
947 Project. FERC Project No. 2246.

948

949 **Tables**

950 Table 1. Dates of snorkel surveys in which *O. tshawytscha* or *O. mykiss* observations
951 were made.

2012	2014	2015
January 3, 4, 5	May 19, 21, 27, 28	January 12, 13, 15, 20
February 8, 9	June 12, 16	March 16, 17, 18
March 7, 8, 9	July 16, 17, 22	April 13, 14, 15
June 13, 14	August 19, 20, 21	May 4, 6, 7
September 5, 6, 7		June 22, 24
		July 8, 9
		August 10

952

953

954

955

956

957

958

959

960

961

962

963

964

965

966 Table 2. Fish counts used for HSC development and bioverification.

		<i>O. tshawytscha</i> fry	<i>O. tshawytscha</i> juvenile	<i>O. mykiss</i> fry	<i>O. mykiss</i> juvenile
HSC development	Observations	212	102	61	43
	Total fish count	5588	1943	925	209
	Adjusted fish count	406.56	185.18	96.75	57.91
Bioverification	Observations	46	37	29	19
	Total fish count	999	500	222	76
	Adjusted fish count	94.16	66.73	43.83	25.88

967

968

969

970

971

972

973

974

975

976

977

978

979

980

981

982

983

984

985

Corrected Final

986 Table 3. HSC values used for each cover type.

Cover type	HSC value
Vegetation	1.00
Bedrock outcrops	0.75
Rip-rap	0.75
Weirs	0.75
Bridge piers	0.75
Bare substrate	0.50

987

988

989

990

991

992

993

994

995

996

997

998

999

1000

1001

1002

1003

1004

1005

Corrected Final

1006 Table 4. Descriptive statistics of microhabitat utilization at HSC observations. Depth
1007 and velocity values are in units of meters and meters per second, respectively.

Statistic	<i>O. tshawytscha</i> fry	<i>O. tshawytscha</i> juvenile	<i>O. mykiss</i> fry	<i>O. mykiss</i> juvenile
Depth mode	0.26	0.58	0.22	0.50
Depth median	0.36	0.55	0.34	0.50
Depth mean	0.45	0.59	0.38	0.58
Depth SD	0.33	0.32	0.20	0.33
Depth range	(0.04-2.10)	(0.06-2.40)	(0.03-0.89)	(0.20-2.00)
Velocity mode	0.00	0.00	0.02	0.02
Velocity median	0.04	0.09	0.04	0.11
Velocity mean	0.09	0.15	0.08	0.18
Velocity SD	0.13	0.17	0.10	0.19
Velocity range	(0.00-0.64)	(0.00-0.79)	(0.00-0.60)	(0.00-0.77)

1008
1009
1010
1011
1012
1013
1014
1015
1016
1017
1018
1019
1020
1021
1022
1023

Corrected Final

1024 Table 5. Mann-Whitney *U* test results comparing CHSI values at utilized and non-
1025 utilized locations.

	<i>O. tshawytscha</i> fry	<i>O. tshawytscha</i> juvenile	<i>O. mykiss</i> fry	<i>O. mykiss</i> juvenile
Median utilized value	0.55	0.66	0.58	0.79
Median non-utilized value	0.36	0.4	0.00	0.15
Difference of medians	0.19	0.26	0.58	0.64
<i>U</i> value	575.5	327	76.5	18
<i>p</i> value	0.0002	0.0001	<0.00001	<0.00001

1026

1027

1028

1029

1030

1031

1032

1033

1034

1035

1036

1037

1038

1039

1040

1041

1042

1043

1044

Corrected Final

1045 Table 6. Bootstrapping statistics from 20 randomly generated datasets, resulting 95%
 1046 confidence thresholds, and FR residuals.

Species and size class	Habitat quality class	Standard deviation	Preference threshold	Avoidance threshold	FR value	FR residual
<i>O. tshawytscha</i> fry	0.00-0.25	0.18	1.36	0.64	0.08	-0.55
	0.25-0.50	0.21	1.42	0.58	1.19	0.00
	0.50-0.75	0.34	1.68	0.32	2.52	0.83
	0.75-1.00	0.84	2.67	-0.67	7.91	5.24
<i>O. tshawytscha</i> juvenile	0.00-0.25	0.27	1.54	0.46	0.14	-0.31
	0.25-0.50	0.22	1.44	0.56	0.26	-0.30
	0.50-0.75	0.35	1.69	0.31	2.47	0.78
	0.75-1.00	0.64	2.28	-0.28	7.49	5.20
<i>O. mykiss</i> fry	0.00-0.25	0.10	1.20	0.80	0.12	-0.68
	0.25-0.50	0.46	1.92	0.08	2.57	0.65
	0.50-0.75	0.73	2.46	-0.46	5.50	3.04
	0.75-1.00	0.74	2.49	-0.49	8.67	6.18
<i>O. mykiss</i> juvenile	0.00-0.25	0.33	1.66	0.34	0.00	-0.34
	0.25-0.50	0.33	1.65	0.35	0.32	-0.03
	0.50-0.75	0.68	2.36	-0.36	1.68	0.00
	0.75-1.00	0.83	2.65	-0.65	7.94	5.29

1047

1048

1049

1050

1051

1052

1053

1054

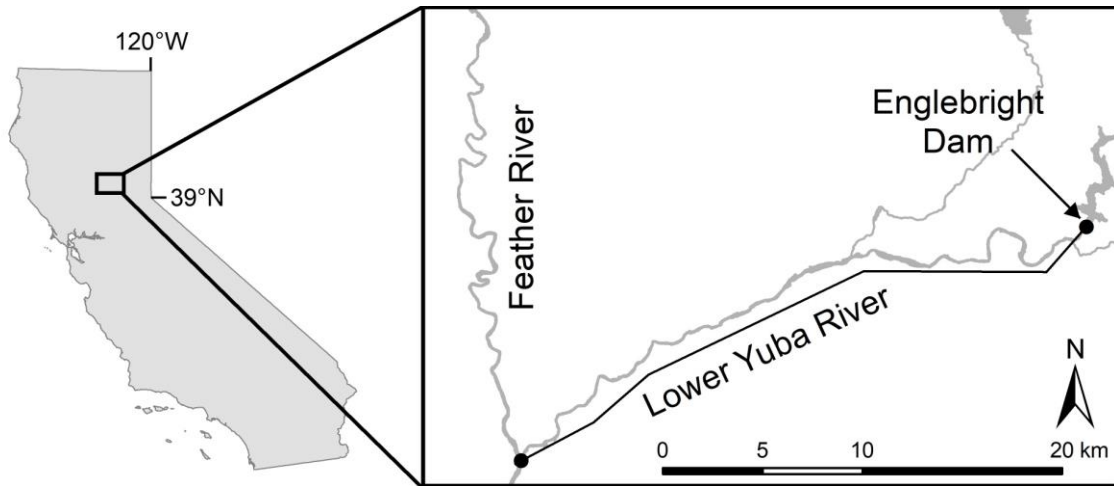
1055

1056

1057

1058

1059 **Figures**



1060

1061 Figure 1. Map of the study location in the lower Yuba River.

1062

1063

1064

1065

1066

1067

1068

1069

1070

1071

1072

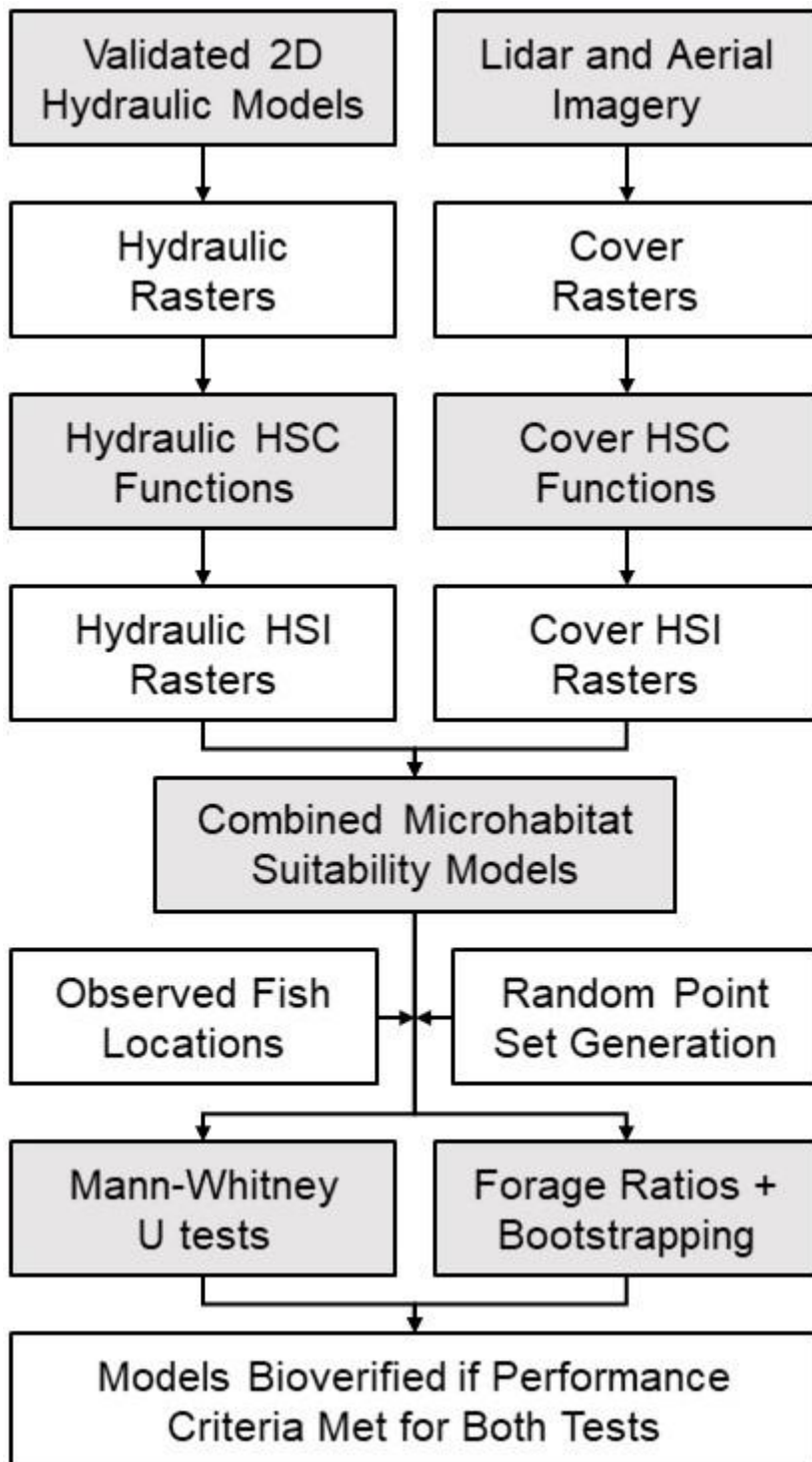
1073

1074

1075

1076

1077



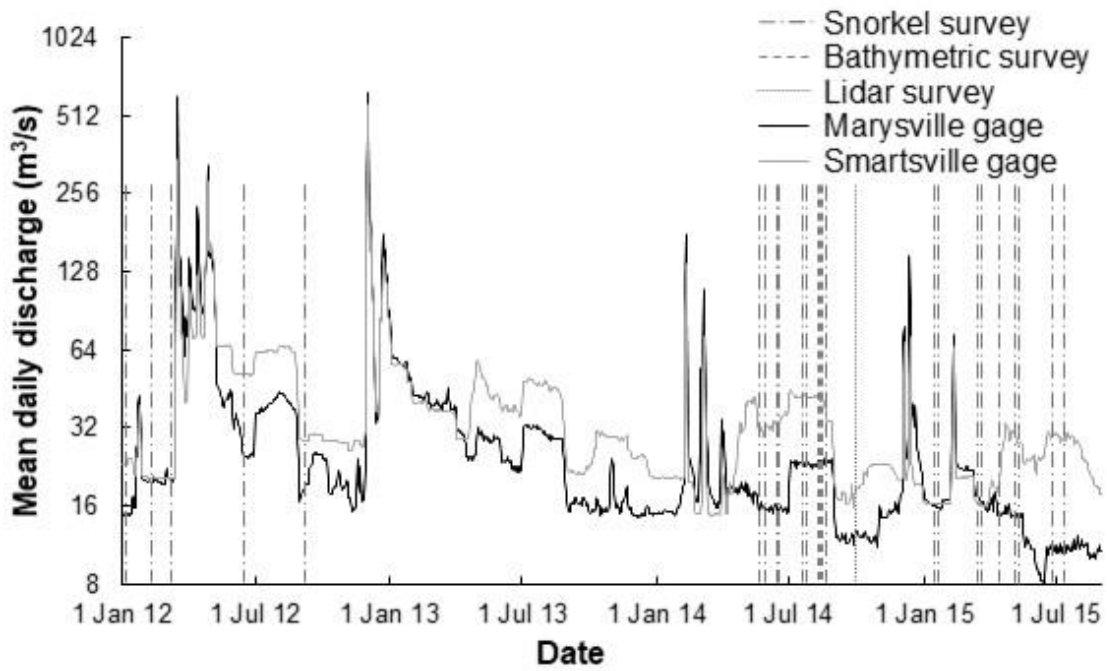
1078

1079 Figure 2. Experimental design for microhabitat suitability model development and
 1080 bioverification with developed HSC functions.

1081

1082

1083



1084

1085 Figure 3. Dates of snorkel and topographic surveys and hydrographs of the LYR
 1086 recorded at the Marysville and Smartsville stream gages throughout the survey period.

1087

1088

1089

1090

1091

1092

1093

1094

1095

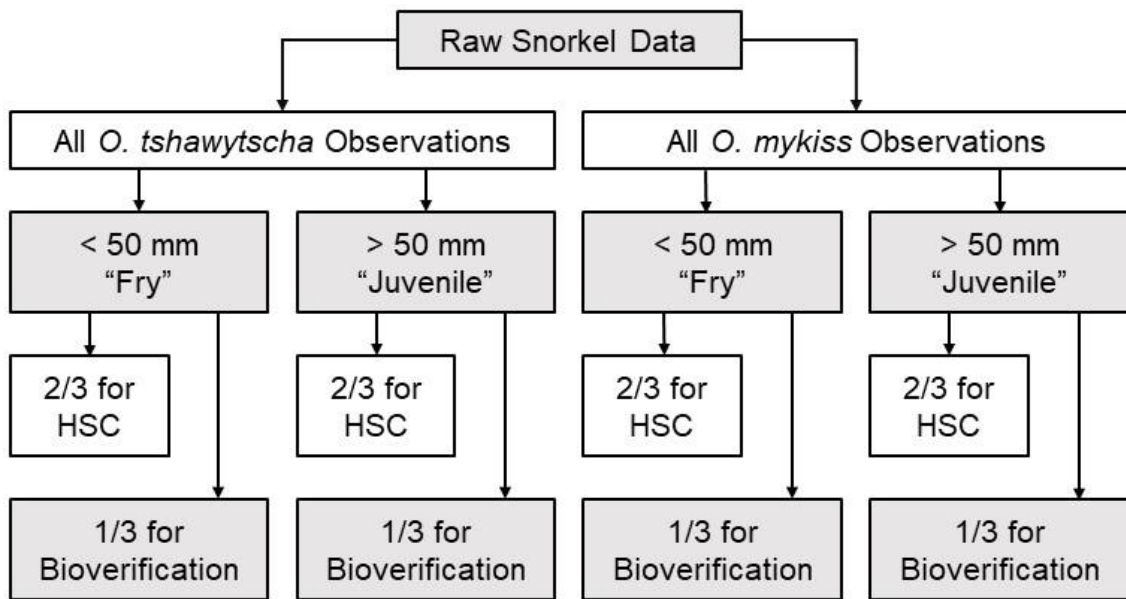
1096

1097

1098

1099

1100



1101

1102 Figure 4. Procedure used to subset snorkel data into independent datasets for developing

1103 HSC functions and bioverification for four species and size classes.

1104

1105

1106

1107

1108

1109

1110

1111

1112

1113

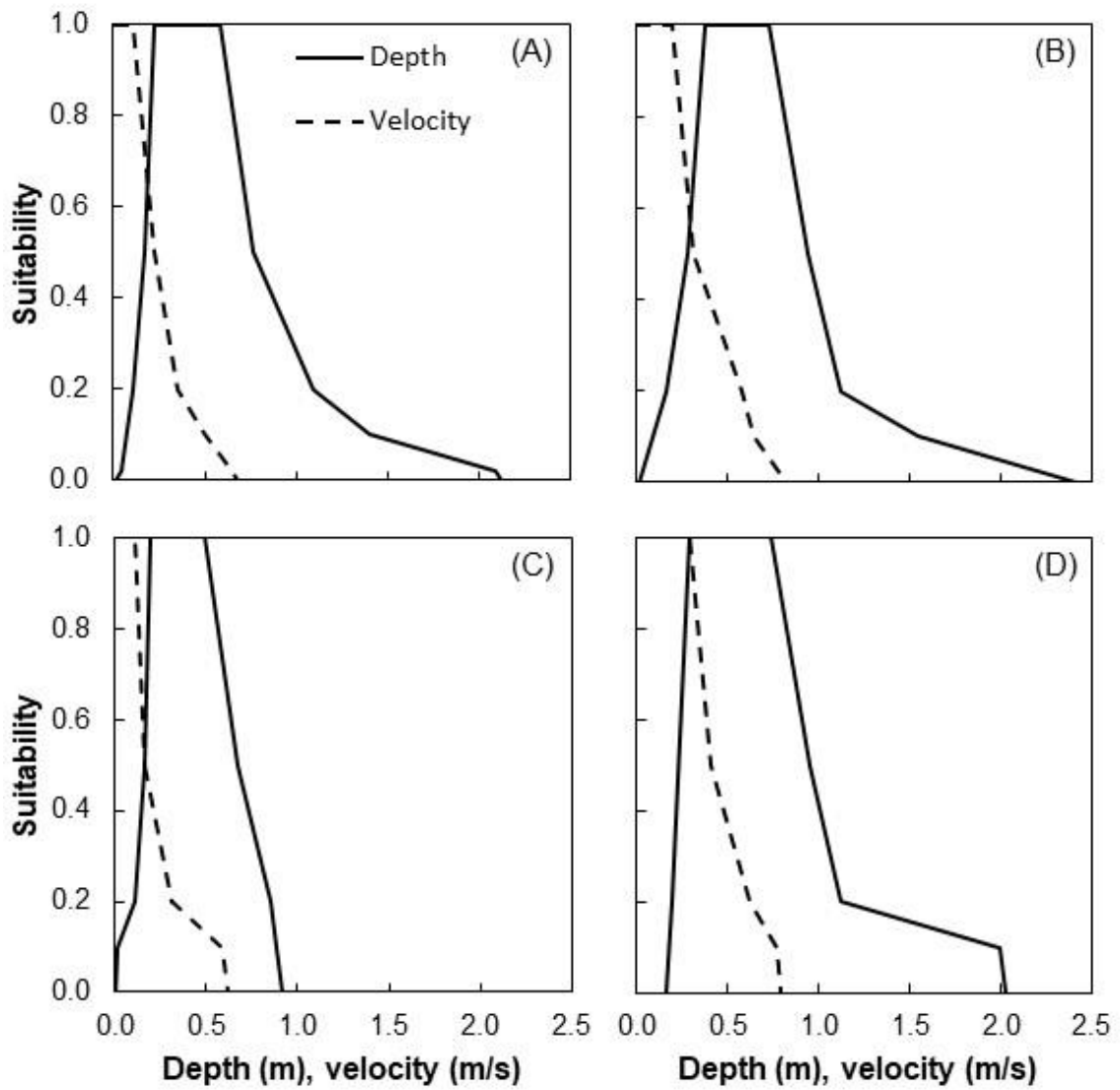
1114

1115

1116

1117

1118



1119

1120 Figure 5. Frequency-based depth and velocity HSC functions for *O. tshawytscha* (A) fry
 1121 and (B) juvenile and *O. mykiss* (C) fry and (D) juvenile.

1122

1123

1124

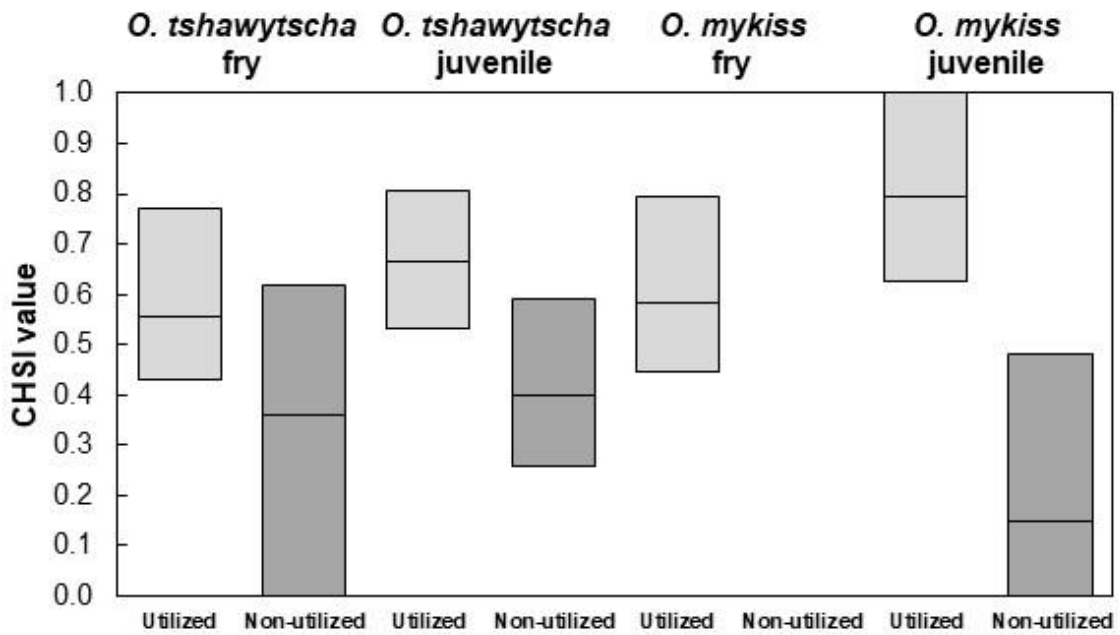
1125

1126

1127

1128

1129



1130

1131 Figure 6. Boxplot of Mann–Whitney U test results comparing CHSI values at utilized
 1132 and non-utilized locations. For *O. mykiss* fry, there is no visible box for non-utilized
 1133 conditions because the interquartile range was zero.

1134

1135

1136

1137

1138

1139

1140

1141

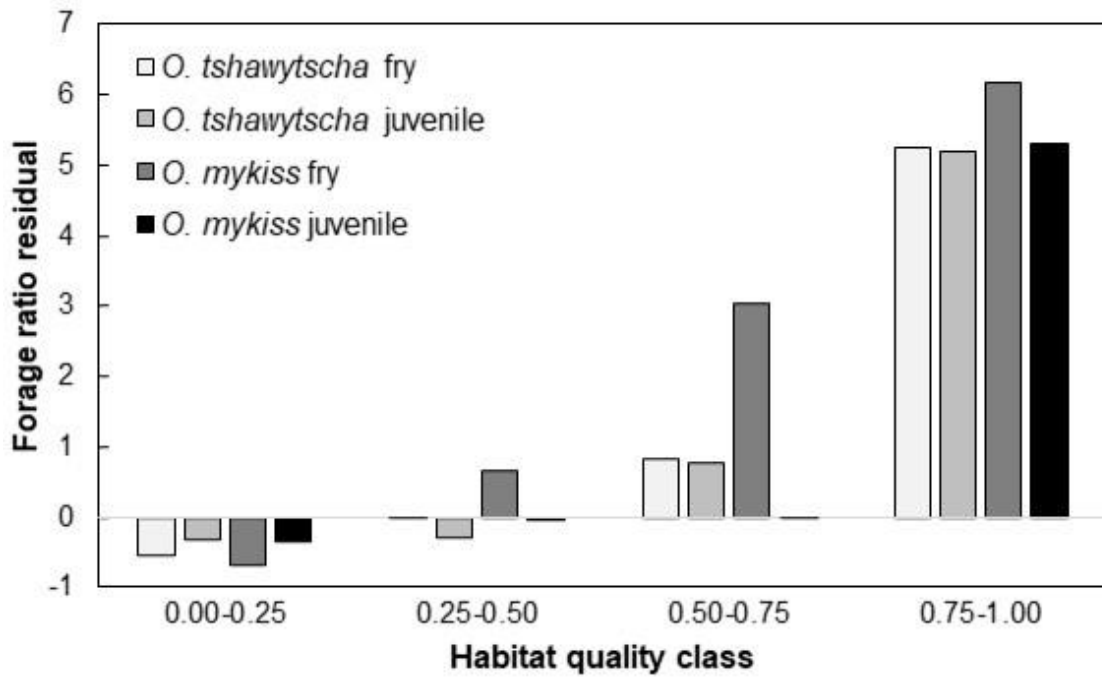
1142

1143

1144

1145

1146



1147

1148 Figure 7. Forage ratio residuals for all four species and size classes.

1149

1150

1151

1152

1153

1154

1155

1156

1157

1158

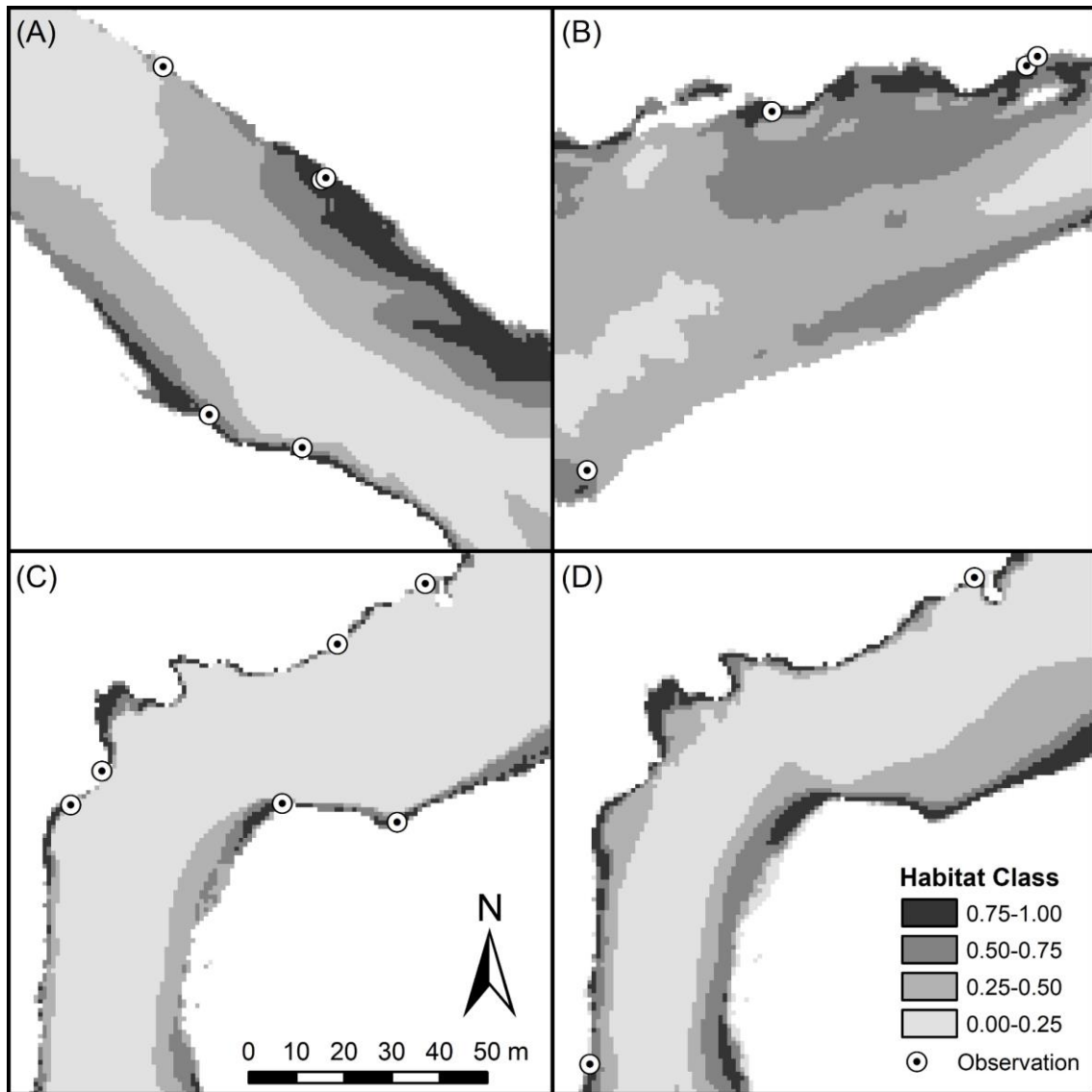
1159

1160

1161

1162

1163



1164

1165 Figure 8. Maps of habitat quality classes for *O. tshawytscha* (A) fry and (B) juvenile

1166 and *O. mykiss* (C) fry and (D) juvenile

1167

1168

1169

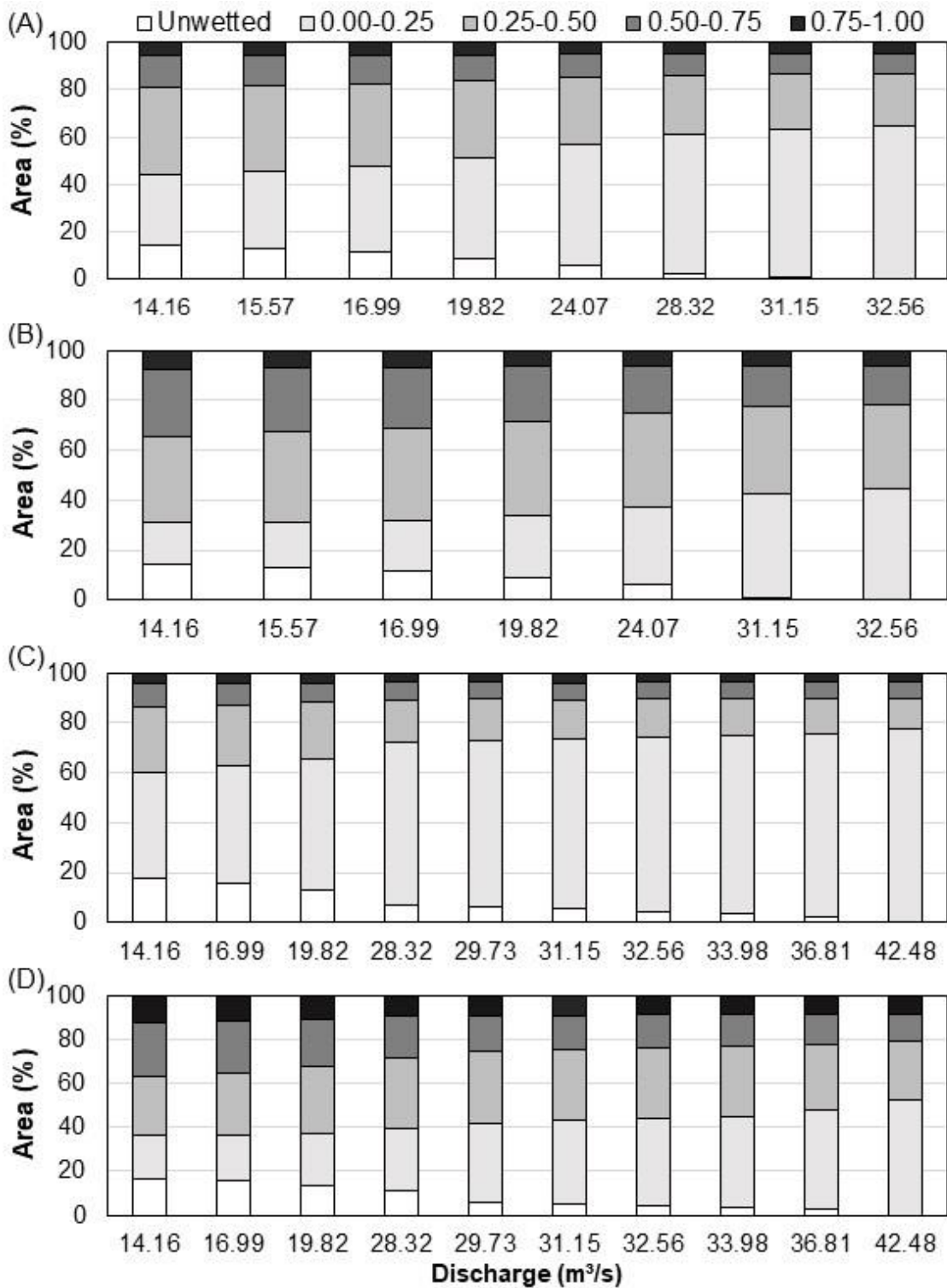
1170

1171

1172

1173

1174



1175

1176 Figure 9. Percentages of area of each habitat quality class at each discharge in which
 1177 bioverification observations were made for *O. tshawytscha* (A) fry and (B) juvenile and
 1178 *O. mykiss* (C) fry and (D) juvenile.